The effect of the Gouy phase in optical-pump-THz-probe spectroscopy

Saima Ahmed, Janne Savolainen, and Peter Hamm[*]

Department of Chemistry, University of Zürich, Winterthurerstrasse 190, 8057 Zurich, Switzerland

[*]*phamm@pci.uzh.ch*

Abstract: We show theoretically as well as experimentally that the Gouy-phase shift, which depends on the exact positioning of a sample in relation to the focus of a probe beam in a pump-probe experiment, may have a pronounced effect on the shape of the pump-probe signal. The effect occurs only when single-cycle probe pulses are used, i.e. when the slowly varying envelope approximation breaks down, while it disappears for multi-cycle pulses. The effect is thus most relevant in THz time-resolved spectroscopy, where such single cycle pulses are most commonly used, but it should not be overlooked also in other spectral regimes when correspondingly short pulses are involved.

References and links

1. B. Ferguson and X. C. Zhang, "Materials for terahertz science and technology," Nat. Mater. **1**, 26–33 (2002).
2. K. Reimann, "Table-top sources of ultrafast THz pulses," Rep. Prog. Phys. **70**, 1597–1632 (2007).
3. J. Faure, J. van Tilborg, R. A. Kaindl, and W. P. Leemans, "Modelling laser based table-top THz sources: Optical rectification, propagation and electro-optic sampling," Opt. Quantum Electron. **36**, 681–697 (2004).
4. Y.-S. Lee, *Principles of Terahertz Science and Technology* (Springer, 2010).
5. M. Theuer, S. S. Harsha, D. Molter, G. Torosyan, and R. Beigang, "Terahertz time-domain spectroscopy of gases, liquids, and solids," Chemphyschem **12**, 2695–2705 (2011).
6. C. A. Schmuttenmaer, "Exploring dynamics in the far-infrared with terahertz spectroscopy," Chem. Rev. **104**, 1759–1779 (2004).
7. E. Pickwell and V. P. Wallace., "Biomedical applications of terahertz technology," J. Phys. D Appl. Phys. **02**, R301 (2009).
8. D. M. Mittleman, R. H. Jacobsen, and M. C. Nuss, "T-ray imaging," IEEE J. Sel. Top. Quantum Electron. **2**(3), 679–692 (1996).
9. K. J. Siebert, T. Loffler, H. Quast, M. Thomson, T. Bauer, R. Leonhardt, S. Czasch, and H. G. Roskos, "All-optoelectronic continuous wave THz imaging for biomedical applications," Phys. Med. Biol. **47**, 3743–3748 (2002).
10. J. Zielbauer and M. Wegener, "Ultrafast optical pump THz-probe spectroscopy on silicon," Appl. Phys. Lett. **68**, 1223 (1996).
11. M. C. Nuss, D. H. Auston, and F. Capasso, "Direct subpicosecond measurement of carrier mobility of photoexcited electrons in gallium arsenide," Phys. Rev. Lett. **58**, 2355–2358 (1987).
12. B. N. Flanders, D. C. Arnett, and N. F. Scherer, "Optical pump-terahertz probe spectroscopy utilizing a cavity-dumped oscillator- driven terahertz spectrometer," IEEE J. Sel. Top. Quantum Electron. **4**, 353–359 (1998).
13. H. Němec, F. Kadlec, and P. Kužel, "Methodology of an optical pump-terahetz probe experiment: An analytical frequency domain approach," J. Chem. Phys. **117**, 8454 (2002).
14. E. Knoesel, M. Bonn, J. Shan, F. Wang, and T. F. Heinz, "Conductivity of solvated electrons in hexane investigated with terahertz time-domain spectroscopy," J. Chem. Phys. **121**, 394–404 (2004).
15. P. A. George, J. Strait, J. Dawlaty, S. Shivaraman, M. Chandrashekhar, F. Rana, and M. G. Spencer, "Ultrafast optical-pump terahertz-probe spectroscopy of the carrier relaxation and recombination dynamics in epitaxial graphene," Nano Lett. **8**, 4248–4251 (2008).

16. M. Breusing, C. Ropers, and T. Elsaesser, "Ultrafast carrier dynamics in graphite," Phys. Rev. Lett. **102**, 086809 (2009).
17. P. U. Jepsen, W. Schairer, I. H. Libon, U. Lemmer, N. Hecker, M. Birkholz, K. Lips, and M. Schall, "Ultrafast carrier trapping in microcrystalline silicon observed in optical pumpterahertz probe measurements," Appl. Phys. Lett. **79**, 1291 (2001).
18. T. Kampfrath, L. Perfetti, F. Schapper, C. Frischkorn, and M. Wolf, "Strongly coupled optical phonons in the ultrafast dynamics of the electronic energy and current relaxation in graphite," Phys. Rev. Lett. **95**, 187403 (2005).
19. D. Polli, M. Rini, S. Wall, R. W. Schoenlein, Y. Tomioka, Y. Tokura, G. Cerullo, and A. Cavalleri, "Coherent orbital waves in the photo-induced insulator-metal dynamics of a magnetoresistive manganite," Nat. Mater. **6**, 643–647 (2007).
20. K. W. Kim, A. Pashkin, H. Schaefer, M. Beyer, M. Porer, T. Wolf, C. Bernhard, J. Demsar, R. Huber, and A. Leitenstorfer, "Ultrafast transient generation of spin-density-wave order in the normal state of bafe2as2 driven by coherent lattice vibrations," Nat. Mater. **11**, 497–501 (2012).
21. G. Haran, W. D. Sun, K. Wynne, and R. M. Hochstrasser, "Femtosecond far-infrared pump-probe spectroscopy: a new tool for studying low-frequency vibrational dynamics in molecular condensed phases," Chem. Phys. Lett. **274**, 365–371 (1997).
22. R. McElroy and K. Wynne, "Ultrafast dipole solvation measured in the far infrared," Phys. Rev. Lett. **79**, 3078–3081 (1997).
23. D. You and P. H. Bucksbaum, "Propagation of half-cycle far infrared pulses," J. Opt. Soc. Am. B **14**, 1651–1655 (1997).
24. C. R. Gouy, "Sur une propriete nouvelle des ondes lumineuses," Acad. Sci. Paris **110**, 1251 (1890).
25. S. Feng, H. G. Winful, and R. W. Hellwarth, "Gouy shift and tempral reshaping of focused single-cycle electromagnetic pulses," Opt. Lett. **23**, 385–387 (1998).
26. P. Kužel, M. A. Khazan, and J. Kroupa, "Spatiotemporal transformations of ultrashort terahertz pulses," J. Opt. Soc. Am. B **16**, 1795–1800 (1999).
27. A. B. Ruffin, J. V. Rudd, J. F. Whitaker, S. Feng, and H. G. Winful, "Direct observation of the Gouy physe shift with single-cycle terahertz pulses," Phys. Rev. Lett. **83**, 3410–3413 (1999).
28. T. Feurer, N. S. Stoyanov, D. W. Ward, and K. A. Nelson, "Direct visualization of the Gouy physe by focusing phonon polaritons," Phys. Rev. Lett. **88**, 257402 (2002).
29. T. Tritschler, K. D. Hof, M. W. Klein, and M. Wegener, "Variation of the carrier-envelope phase of few-cycle laser pulses owing to the Gouy phase: a solid-state-based measurement," Opt. Lett. **30**, 753–755 (2005).
30. L. Zhang, H. Zhong, K. Mu, C. Zhang, and Y. Zhao, "Phase characterization in broadband THz wave detection through field-induced second harmonic generation," Opt. Express **20**, 75–80 (2012).
31. R. W. Boyd, *Nonlinear Optics* (Academic, 1992).
32. N. Lastzka and R. Schnabel, "The Gouy phase shift in nonlinear interactions of waves," Opt. Express **15**, 7211–7217 (2007).
33. C.-Y. Chung, J. Hsu, S. Mukamel, and E. O. Potma, "Controlling stimulated coherent spectroscopy and microscopy by a position-dependent phase," Phys. Rev. A **87**, 033833 (2013).
34. J. T. Kindt and C. A. Schmuttenmaer, "Theory for determination of the low-frequency time-dependent response function in liquids using time-resolved terahertz pulse spectroscopy," J. Chem. Phys. **110**, 8589 (1999).
35. P. Kužel, H. Němec, and F. Kadlec, "Propagation of THz pulses in photoexcited media: Analytical theory for layered systems," J. Chem. Phys. **127**, 024506 (2007).
36. P. Kužel, H. Němec, F. Kadlec, and C. Kadlec, "Gouy shift correction for highly accurate refractive index retrieval in time-domain terahertz spectroscopy," Opt. Express **18**, 15338–15348 (2010).
37. J. Savolainen, S. Ahmed, and P. Hamm, "2D Raman-Thz spectroscopy of water," Proc. Natl. Acad. Sci. U. S. A. **110**, 20402–20407 (2013).
38. P. Hamm and J. Savolainen, "2D-Raman-THz spectroscopy of water: Theory," J. Chem. Phys. **136**, 094516 (2012).
39. F. Krausz and M. Ivanov, "Attosecond physics," Rev. Mod. Phys. **81**, 163–234 (2009).
40. L. Gallmann, J. Herrmann, R. Locher, M. Sabbar, A. Ludwig, M. Lucchini, and U. Keller, "Resolving intraatomic electron dynamics with attosecond transient absorption spectroscopy," Molecular Physics, in press, DOI:10.1080/00268976.2013.799298 (2013).
41. N. Shivaram, A. Roberts, L. Xu, and A. Sandhu, "In situ spatial mapping of Gouy phase slip for high-detail attosecond pumpprobe measurements," Opt. Lett. **35**, 3312–3314 (2010).
42. G. Cerullo, M. Nisoli, S. Stagira, and S. D. Silvestri, "Sub-8-fs pulses from an ultrabroadband optical parametric amplifier in the visible," Opt. Lett. **23**, 1283-1285 (1998).
43. D. Herrmann, C. Homann, R. Tautz, M. Scharrer, P. S. J. Russell, F. Krausz, L. Veisz, and E. Riedle, "Approaching the full octave: Noncollinear optical parametric chirped pulse amplification with two-color pumping," Opt. Express **18**, 18752–18762 (2010).
44. T. Kobayashi, J. Liu, and K. Okamura, "Applications of parametric processes to high-quality multicolour ultrashort pulses, pulse cleaning and cep stable sub-3fs pulse," J. Phys. B At. Mol. Opt. Phys. **45**, 074005 (2012).

45. P. B. Petersen and A. Tokmakoff, "Source for ultrafast continuum infrared and terahertz radiation," Opt. Lett. **35**, 1962–1964 (2010).
46. M. Cheng, A. Reynolds, H. Widgren, and M. Khalil, "Generation of tunable octave-spanning mid-infrared pulses by filamentation in gas media," Opt. Lett. **37**, 1787–1789 (2012).

1. Introduction

Over the last two decades, there has been a tremendous development in THz technology [1–4] in different areas of science in both spectroscopy [5, 6] and imaging [7–9]. Optical pump-THz-probe spectroscopy has been widely applied to study e.g. the ultrafast carrier dynamics in various materials [10–16], phonon dynamics [17,18] and other excitations in strongly correlated materials [19,20], as well as low frequency vibrational dynamics in molecular liquids [6,21,22].

Short THz pulses change spatially and temporally as they propagate through a measurement setup [23]. One such important process is the Gouy phase shift [24, 25]. That is, when a laser pulse travels through a focus, it experiences a phase shift from $+\pi/2$ before the focus, 0 in the focus, and $-\pi/2$ after the focus, and in fact THz pulses have been used elegantly to visualize the effect [26–30]. It is widely recognized that the Gouy phase shift may play a role in nonlinear optics [31, 32] as well as in nonlinear spectroscopy, e.g. when phase-sensitive heterodyning is applied [33]. In the present paper, we demonstrate that the Gouy phase shift can also have a pronounced effect on the outcome of optical pump-THz-probe experiments. Despite the fact that many such experiments have been performed in the past [10–22], we are not aware of any discussion of that effect.

We consider a prototype optical-pump-THZ-probe experiment as schematically shown in Fig. 1. A short THz pulse is generated by optical rectification in a non-linear crystal, imaged by some imaging optics onto the sample, where it is overlapped with an optical pump-pulse, and the generated 3rd-order field $E^{(3)}(t)$ is imaged onto the detection crystal. The nonlinear interaction in the sample can be describe by the usual convolution of the laser pulses with a system response function $R(t_1, t_2)$:

$$P^{(3)}(t) \propto \int_0^\infty \int_0^\infty E_{THz}(t - t_2) I_{pu}(t - t_1) R(t_1, t_2) dt_1 dt_2 \qquad (1)$$

with $I_{pu}(t) = |E_{pu}(t)|^2$ the intensity profile of the pump pulse. Deducing the system response function $R(t_1, t_2)$, which is ultimately what we want to measure, effectively requires a deconvolution of the measured field [13, 34, 35], which in turns requires that we very accurately know the THz pulse $E_{THz}(t)$ at the sample position including its phase. This is where the Gouy phase shift comes into play.

In a idealized realization of Fig. 1, the Gouy phase shift would not matter since both generation and detection crystal as well as the sample are in the focus of the imaging optics and typically are thin, so the Gouy phase is the same apart from alternating minus signs in all three positions. However, since one wants to achieve high intensities of the pump-light in the sample to explore its pump-probe response, the THz pulse is often imaged with high-aperture optics to achieve a small focus. The Gouy phase changes on a scale that equals the Rayleigh length, which in turns is of the order of the wavelength of the THz light if the aperture approaches 1. Consequently, the positioning of the crystals and the sample is critical within a few 100 μm for a typical THz experiment. While the alignment of the crystals can easily be checked by measuring the Gouy phase of the THz pulse itself (which also enters the detection crystal), the exact positioning of the sample in between is less easy to determine.

One is tempted to assume that the exact positioning of the sample does not matter, since a "wrong" Gouy phase in $E_{THz}(t)$ is compensated by the corresponding Gouy phase that the emitted field accumulates on its way from the sample to the detection crystal. Although the
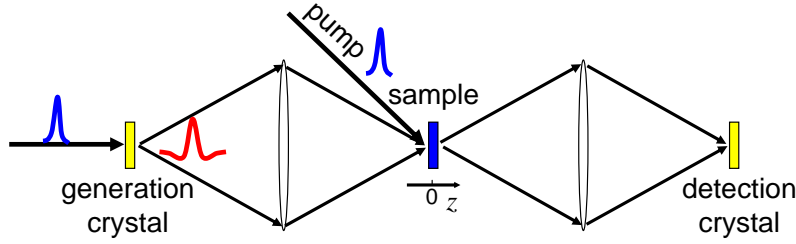
Fig. 1. Scheme of a optical-pump-THz-probe experiment. The displacement z is measured relative to the middle focus.

Gouy phase is a propagation effect, whose explanation requires the solution of the 3D Maxwell equations, it can be described by adding a phase ϕ to a propagating field in a 1D description. Hence, one might think that one can add a phase factor $e^{i\phi}$ to the input THz pulse in Eq. (1)

$$e^{i\phi}P^{(3)}(t) \propto \int_0^\infty \int_0^\infty e^{i\phi}E_{THz}(t-t_2)I_{pu}(t-t_1)R(t_1,t_2)dt_1dt_2 \qquad (2)$$

which of course can be pulled in front of the integral, and hence would cancel with a compensating phase $e^{-i\phi}$ for the emitted field. However, physical electric fields are real-valued. Using complex electric fields is a mathematical trick that simplifies many calculations, but is rigorously correct only as long as linear optics is considered. Despite the fact that the THz field $E_{THz}(t)$ enters in Eq. (1) in a linear fashion, the operation as a whole is nonlinear, which can be seen from the fact that the multiplication with a potentially much shorter pump-pulse $I_{pu}(t)$ can generate new frequency components in $P^{(3)}(t)$. Adding a phase factor in Eq. (2) inevitably results in a complex field which can be done only in certain limits.

For very short pulses, it is no longer meaningful to write them as an envelope times a carrier frequency:

$$E(t) = E_0(t)\cos(\omega_0 t) \qquad (3)$$

which can be seen for example from the fact that such a pulse would have a non-vanishing amplitude at zero frequency (i.e. a DC component, which it cannot have in the far-field) whenever the time duration of $E_0(t)$ gets in the same order of magnitude as $1/\omega_0$. Consequently, one can also not introduce a phase by simply writing:

$$E(t) = E_0(t)\cos(\omega_0 t + \phi) \qquad (4)$$

Alternatively, one may use a close analog of the Hilbert transformation to do so (while the common definition of the Hilbert transformation transforms a real field into its imaginary counterpart $\Re E(t) \to \Im E(t)$, we consider here the transformation of the real field into the complex field $\Re E(t) \to \Re E(t) + i\Im E(t)$). That is, the field is Fourier-transformed into the frequency domain, the negative frequencies are zeroed, and the field is Fourier-transformed back into the time-domain, which will result in a complex-valued representation of the field (in the following we will use a tilde to indicate a field is complex). The phase factor may then be added and the real part be taken:

$$E(t) \xrightarrow{FT} E(\omega) \to \Theta(\omega)E(\omega) \xrightarrow{FT^{-1}} \tilde{E}(t) \to \Re(e^{i\phi}\tilde{E}(t)) \qquad (5)$$

where $\Theta(\omega)$ is the Heaviside step function. Not that this sequence of operations is not equivalent to Eq. (4), if the slowing varying envelope approximations doesn't apply.

The operations Eq. (1) and Eq. (5) do not commute. If they would commute, then one could first transform $E_{THz}(t)$ into a complex field $\tilde{E}_{THz}(t)$, plug it into Eq. (1) including the phase factor $e^{i\phi}$, add a phase factor $e^{-i\phi}$ to the generated 3-order polarization $\tilde{P}^{(3)}(t)$ in order to describe the compensating Gouy-phase, which then would cancel:

$$E_{THz}(t) \to e^{i\phi}\tilde{E}_{THz}(t) \xrightarrow{Eq.(1)} e^{i\phi}\tilde{P}^{(3)}(t) \to e^{-i\phi}e^{i\phi}\tilde{P}^{(3)}(t) \to \Re(\tilde{P}^{(3)}(t)) \tag{6}$$

The correct treatment of the problem first transforms $E_{THz}(t)$ into a complex field $\tilde{E}_{THz}(t)$, adds a phase factor, but then plugs only the real part $\Re(e^{i\phi}\tilde{E}_{THz}(t))$ into Eq. (1), and finally repeats the compensating phase shift for $P^{(3)}(t)$:

$$E_{THz}(t) \to Re(e^{i\phi}\tilde{E}_{THz}(t)) \xrightarrow{Eq.(1)} P^{(3)}(t) \to e^{-i\phi}\tilde{P}^{(3)}(t) \to \Re(e^{-i\phi}\tilde{P}^{(3)}(t)) \tag{7}$$

Both lines of operations do not necessarily reveal the same result.

It is instructive to see in the next section why and how a "wrong" Gouy phase is indeed compensated in linear response. We will furthermore show that a Gouy phase is still compensated also in a pump-probe response as long as multi-cycle pulses are used, which is why this problem is not relevant for most applications of femtosecond spectroscopy. However, in THz pump-probe spectroscopy, where single-cycle pulses are most common, the Gouy-phase has to be taken into account for a quantitative interpretation of the data. To that end, we will show both theoretically and experimentally that the outcome of a optical-pump-THz-probe experiment does in fact depend on the exact position of the sample relative to the focus.

2. Linear response

In the most simple approximation, linear response is described as:

$$P^{(1)}(t) \propto \int_0^\infty E_{THz}(t-t_1)R(t_1)dt_1 \tag{8}$$

As the integral is a convolution of 1D functions, the convolution theorem applies and it is advantageous to treat the problem in frequency domain:

$$\tilde{P}^{(1)}(\omega) \propto \tilde{E}_{THz}(\omega)\tilde{R}(\omega) \tag{9}$$

where $\tilde{E}(\omega)$ and $\tilde{R}(\omega)$ are the Fourier transformations of the corresponding functions in Eq. (8). Along the lines of Eq. (5), the negative frequencies are then zeroed:

$$\tilde{P}^{(1)}(\omega) \propto \Theta(\omega)\tilde{E}_{THz}(\omega)\tilde{R}(\omega) \tag{10}$$

All operations in Eq. (10) are simple products in frequency domain that of course do commute, and hence they will also commute in the time domain. Consequently, the equivalents of Eqs. (6) and (7) do indeed reveal the same results and a Gouy phase in the input field will be compensated by that of the emitted field, so the measured linear response does of course *not* depend on the exact positioning of the sample in the focus in Fig. 1.

It should however be added that when including the fact that a THz pulse undergoes multiple reflections at the sample surfaces, then different terms with changing Gouy phases add up (an effect that goes beyond Eq. (8)) and the Gouy phase has in fact a subtle effect even on the linear response [36]. This is yet another effect of the Gouy phase on spectroscopy that is however distinctively different from the one discussed here.
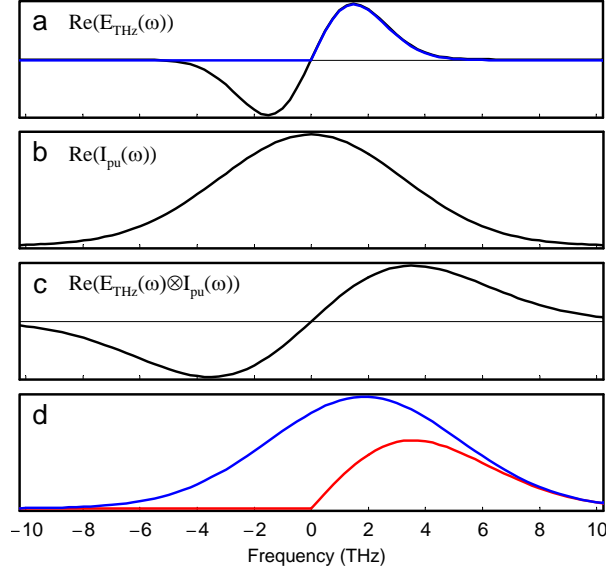
Fig. 2. (a) Spectrum of the THz pulse $\tilde{E}_{THz}(\omega)$ (Eq. (14), black) and with negative frequencies zeroed (blue). (b) Fourier transformation of the pump pulse intensity profile $\tilde{I}_{pu}(\omega)$ (Eq. (15)). (c) Convolution $\tilde{E}_{THz}(\omega) \otimes \tilde{I}_{pu}(\omega)$ and (d) convolution with zeroing negative frequencies of the THz pulse $\tilde{E}_{THz}(\omega)$ before the convolution (blue) and after the convolution (red). The pump-probe delay between the center of both pulses was set to $t_{pp} = 0$.

3. Pump-probe response

To simplify matters, we first consider a system response function that is faster than any other timescale of the system (e.g. a polarisibility that is exclusively electronic), so that it can be approximated as a δ-function:

$$R(t_1, t_2) = \delta(t_1)\delta(t_2) \tag{11}$$

In this case, Eq. (1) reduces to:

$$P^{(3)}(t) \propto E_{THz}(t) I_{pu}(t), \tag{12}$$

It is a simple product in time domain, so it will be a convolution in frequency domain:

$$\tilde{P}^{(3)}(\omega) \propto \tilde{E}_{THz}(\omega) \otimes \tilde{I}_{pu}(\omega). \tag{13}$$

Note that here $\tilde{I}_{pu}(\omega)$ is the Fourier transformation of the intensity profile of the pump pulse, and not that of its field, and thus it is centered around $\omega = 0$. Figure 2 shows the result of that convolution for a typical situation in a THz pump-probe experiment. To that end, we assumed a half-cycle THz pulse (see Fig. 3, top-middle panel):

$$E_{THz}(t) \propto \Re \int_0^\infty \omega e^{-\tau_1^2 \omega^2/4} e^{i\omega t} d\omega \tag{14}$$

where $\tau_1 = 150$ fs is a measure of the pulse duration (the pulse is constructed as the time-derivative of a generating Gaussian pulse together with a $\pi/2$ phase shift). For the pump pulse,
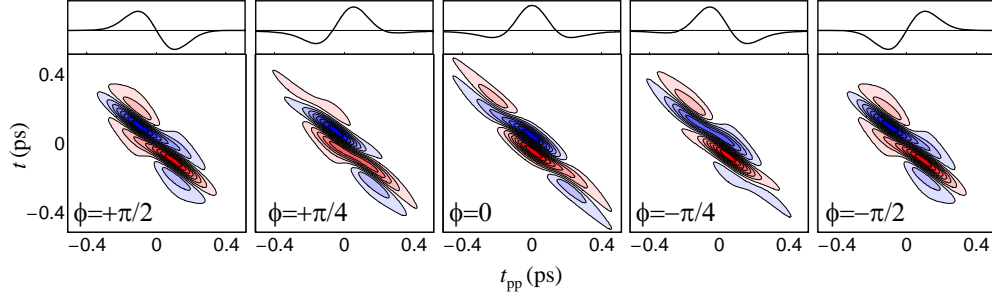
Fig. 3. Outcome of a hypothetical pump probe experiment of a sample with infinitesimally fast response function as a function of THz detection time t, pump-probe delay time t_{pp} between the center of both pulses, and the Gouy-phase error of the sample. Red and blue depict positive and negative fields, respectively. The top panels show the corresponding input THz pulse $E_{THz}(t)$.

we assumed a Gaussian pulse:

$$I_{pu}(t) \propto e^{-t^2/\tau_2^2} \tag{15}$$

with $\tau_2 = 70$ fs. Figure 2(a), black, shows the spectrum of the resulting THz pulse $\tilde{E}_{THz}(\omega)$, Fig. 2(b) that of the pump pulse intensity profile $\tilde{I}_{pu}(\omega)$ and Fig. 2(c) the convolution Eq. (13). Applying the Hilbert transformation after the convolution, which simply zeros the negative frequencies (Fig. 2(d), red), obviously gives a different result as compared to applying the Hilbert transformation before the convolution. The latter is shown in Fig. 2(d), blue line, which results from the convolution of the blue line in Fig. 2(a) with Fig. 2(b). In other words, the Hilbert transformation and the nonlinear interaction in Eq. (1) do not commute:

$$\Theta(\omega)\left(\tilde{E}_{THz}(\omega) \otimes \tilde{I}_{pu}(\omega)\right) \neq \left(\Theta(\omega)\tilde{E}_{THz}(\omega)\right) \otimes \tilde{I}_{pu}(\omega) \tag{16}$$

Figure 3 shows the effect of a Gouy phase for a hypothetical pump probe experiment of a sample with infinitesimally fast response function (Eq. (11)), using Eqs. (12), (14) and (15) together with

$$E^{(3)}(t) \propto \frac{dP^{(3)}(t)}{dt} \tag{17}$$

which connects the emitted 3rd-order field to the 3rd-order polarization in the most simple case when dispersion and absorption can be neglected and the process is quasi-phasematched [13, 34, 35]. In addition, a Gouy phase ϕ is added along the lines of Eq. (7). These plots can be considered to be the instrument response of such an experiment. Identical responses are obtained for Gouy phases $\phi = +\pi/2$ and $\phi = -\pi/2$, which however clearly differs from that for $\phi = 0$. It should be noted that the effects are the stronger the shorter the pump pulse duration is compared to the THz pulse duration.

If, on the other hand, we write the probe pulse as a carrier wave times a pulse envelope:

$$E_{THz}(t) = \cos(\omega_0 t)e^{-t^2/\tau_1^2} \tag{18}$$

with $\omega_0 = 20$ THz (and leave the pump pulse as in Eq. (15)), the situation shown in Fig. 4 is obtained. In this case, the positive frequency and negative frequency contribution of $\tilde{E}_{THz}(\omega)$
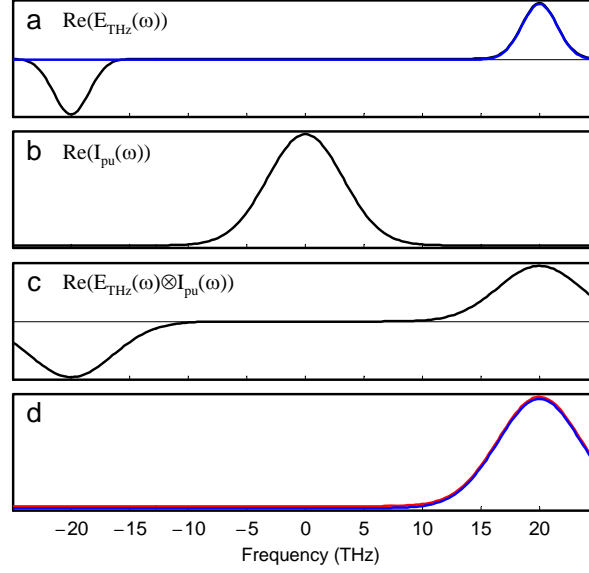
Fig. 4. Same as in Fig. 2, but for a THz pulse according to Eq. (18). The red line in (d) has been offset a little bit to make it visible.

do not overlap with $\tilde{I}_{pu}(\omega)$, which is centered around $\omega = 0$, and Hilbert transformation and the nonlinear interaction in Eq. (1) do commute to a very good approximation (compare red and blue line in Fig. 4(d), which is hardly different):

$$\Theta(\omega)\left(\tilde{E}_{THz}(\omega) \otimes \tilde{I}_{pu}(\omega)\right) \approx \left(\Theta(\omega)\tilde{E}_{THz}(\omega)\right) \otimes \tilde{I}_{pu}(\omega) \tag{19}$$

In this case, a Gouy phase in the input field will be compensated by that of an outgoing field since Eq. (6) would be correct. We see that it is the spectrum of a typical THz pulse that covers all frequencies down to zero, or in other words, the break-down of the slowly varying envelope approximation, that makes the difference to "normal" femtosecond spectroscopy.

Finally, we consider a general response function that is not necessarily infinitesimally fast. To that end, we start with an auxiliary function

$$P'(t',t'') \propto \int_0^\infty \int_0^\infty E_{THz}(t''-t_2)I_{pu}(t'-t_1)R(t_1,t_2)dt_1dt_2 \tag{20}$$

which is in fact a 2D convolution of the response function with the laser pulses. Hence, we again can switch to the frequency domain

$$\tilde{P}'(\omega',\omega'') \propto \tilde{E}_{THz}(\omega'')\tilde{I}_{pu}(\omega')\tilde{R}(\omega',\omega'') \tag{21}$$

The fact that we need to evaluate $P'(t',t'')$ only for $t' = t''$, $P(t) = P'(t,t)$, is equivalent to

$$\tilde{P}(\omega) \propto \int_{-\infty}^\infty \tilde{P}'(\omega',\omega-\omega')d\omega' \tag{22}$$

in the frequency domain. This expression is tedious to visualize, but in essence the argument of Fig. 2 *versus* Fig. 4 remains.

4. Experimental verification

To demonstrate the effect of the Gouy phase on the outcome of a concrete pump-probe experiment, we use the Raman-pump-THz probe response of water as an illustrative example. The relevance of such an experiment for water structure and dynamics has been explored in detail in a separate publication [37]. To give a brief motivation of that experiment, a first Raman interaction induced by a 800 nm pulse excites a coherence in low-frequency intermolecular modes of the hydrogen-bonded water network that is switched into another coherence by the subsequent THz pulse and finally read out by the emission of a THz field. The experiment has been termed 2D-Raman-THZ-probe spectroscopy, as it allows one to measure correlations among the various degrees of freedom of water, and indeed, a very short lived THz photon-echo has been observed. In Ref. [37] a full 2D data set in analogy to Fig. 3 has been measured, while we show here only 1D scans along the pump-probe delay time t_{pp} with the detection time t kept fixed to the position where the signal is maximal.

The experiment was performed with a optical-pump-THz-probe setup that is similar to many such implementations described in the literature [10–22], and that is introduced in detail in Ref. [37]. In brief, a half-cycled THz pulse was generated in a 100 μm GaP [110] crystal by optical rectification [3, 4] and was imaged by a single home-machined elliptical mirror ($2f$=83 mm) onto a 40 μm thick water jet, which was pumped by an intense 800 nm pulse through a non-resonant Raman process. Due to the high-aperture of the elliptical mirror ($A \approx 1$), the THz pulse could be focused in a transform-limited manner onto a spot of diameter ≈ 240 μm. The generated 3rd-order field was imaged by another elliptical mirror onto a second GaP crystal for electro-optical sampling. The beam size of the Raman-pump pulse (diameter 300 μm) was adjusted to match that of the THz pulse in the focus. Due to its much shorter wavelength, the beam size can be considered to be essentially constant in the range around the focus which is relevant for the present discussion. Alternatively, the detection crystal was put at the sample position to measure the input THz field $E_{THz}(t)$ directly. In that case, the positioning of the detection crystal relative to the water jet was measured with the help of a confocal chromatic measurement sensor (ConfocalDT, micro-epsilon) that provides a few micrometers resolution.

Figure 5, top row, shows the input THz pulse at various positions relative to the focus from z=-500 μm to z=500 μm, where we assumed the focus z=0 μm to be the position where the pulse is symmetric (the displacement z is defined in Fig. 1). As we move away from the focus in both directions, the phase of the THz pulse changes. The red lines in Fig. 5, top row, show the THz pulses measured at the various positions, while the black dotted lines take the pulse at z=0 μm and add a phase ϕ that was varied to give the best match with the red lines. As can be seen, a simple phase shift can very well describe the Gouy phase of the THz pulse as the crystal is moved through the focus. Between z=-500 μm to z=500 μm, the Gouy phase changes from $\approx 0.3\pi$ to $\approx -0.3\pi$. The fact that a simple Gouy phase shift can indeed describe the effect of moving the detection crystal through the focus quite well proves that effects of a changing frequency-dependent overlap between pump pulse and the THz probe pulse do play only a minor role, owing to the high-aperture THz optics (red and black dotted lines in Fig. 5 would match exactly if the spectral amplitude would not change at all.)

Figure 5, bottom row, shows the effect of the Gouy phase shift on the resulting Raman-pump-THz-probe signal. Between the various measurements of Fig. 5, bottom row, nothing has been touched in the experimental setup except of the crystal or the jet that has been moved by the indicated distance. As a trivial result, when the water jet is moved off-focus, the signal size diminishes due to the smaller spatial overlap between pump and probe pulses. More importantly, however, the shape of the response changes quite a bit, significantly more than the small deviations between red and black dotted lines in Fig. 5, top row, would suggest. For example, while
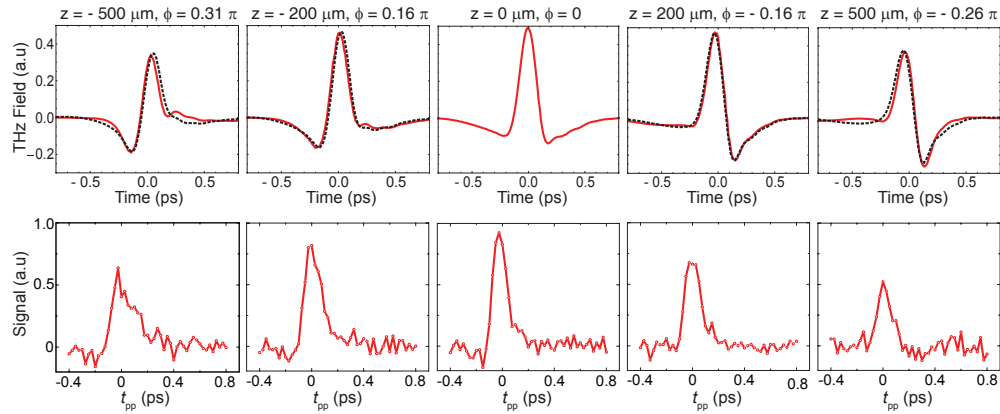
Fig. 5. Top panels: THz pulses (red) at various positions relative to the focus from -500 μm to +500 μm. The phases ϕ of these pulses have been estimated by taking the pulse at z=0 μm and adding a phase that has been varied to give the best fit (black dotted lines). Bottom panels: Raman-pump-THz-probe signal from water at various z-positions in dependence of pump-probe delay t_{pp} between the peaks of the Raman-pump and the THz probe pulse. The detection time t was kept fixed at 50 fs relative to the peak of the transmitted THz pulse, where the signal is maximal.

a quite sharp response is found at z=0 μm, the signal at z=-500 μm might be misinterpreted as relatively slow decay. Interestingly, it is these z=-500 μm data which exhibit the slowest decay, despite the fact that the THz pulse is slightly shorter (Fig. 5, top row) due to a somewhat smaller overlap of the lower frequency components when being off-focus. Hence the effect is opposite to what would be expected if a frequency-dependent overlap would be the origin.

Despite the fact that the Raman-pump-THz probe response of water includes a relatively large instantaneous contribution, originating from the electronic polarisibility and fast librational motions, the cuts in Fig. 5, bottom row, cannot be directly compared to Fig. 3, because slower components from hydrogen bond rearrangements exist in the water response function as well [37]. Nonetheless, Fig. 5, bottom row, clearly shows that the exact positioning of the sample does matter for the outcome of optical-pump-THz-probe experiments, for the reasons discussed in the previous section.

5. Discussion and conclusion

The Raman-pump-THz probe response of water is quite short lived [37, 38]. That is, the response function $R(t_1, t_2)$ in Eq. (1) indeed adds new frequency components to the emitted THz field that might not be present in the input field E_{THz}. This is the situation when the effect discussed in this paper is most relevant. When the response function varies slowly, then Eq. (1) represents a quasi-linear response which does not change during the duration of the THz pulse, in which case effectively the situation described in Sec. 2 would apply.

In conclusion, we discussed the effect of the Gouy phase on optical-pump-THz-probe experiments. In particular when high-aperture imaging optics is used, great care should be taken to precisely position the generation and detection crystals as well as the sample in their corresponding foci, in order to avoid severe perturbations of the measured signal. We have shown that the effect is related to the single-cycle pulses typically used in THz spectroscopy, whose spectral width is comparable to their center frequency, so that they span everything down to zero frequency. The effect is not relevant in most pump-probe studies in the visible or mid-IR

spectral range, where typically multi-cycle pulses are used. But when very short pulses are employed in attosecond spectroscopy [39–41], or in the visible [42–44] or mid-IR [45,46] spectral range, the effect should not be overlooked.

Acknowledgments